Experimentally feasible generation protocol for polarized hybrid entanglement

Shujing Li, Hongmei Yan, Yaya He, and Hai Wang*

The State Key Laboratory of Quantum Optics and Quantum Optics Devices, Collaborative Innovation Center of Extreme Optics, Institute of Opto-Electronics, Shanxi University, Taiyuan 030006, People's Republic of China

(Received 8 June 2018; published 31 August 2018)

We propose a scheme to generate polarized hybrid entanglement in the form of $|H\rangle|\alpha\rangle + |V\rangle|-\alpha\rangle$ by interference between a superposition of coherent states and a polarization entangled photon pair. In the scheme two sets of interferences with perpendicular polarizations are designed to erase "which path" information. The joint output fields of the two sets of interferences are used to herald the generation of the polarized hybrid entanglement. The advantage of the protocol is its experimental feasibility since it not only realizes effective interference but also retains the polarization information in the output fields of interferences. We also analyze the effect of imperfect experimental conditions on the generated hybrid state, including inefficiency on-off single-photon detectors with dark counts and available approximate resource states. The theoretical analysis shows that the fidelity of the heralded hybrid state with small amplitude can be maintained at a high level under actual experimental conditions.

DOI: 10.1103/PhysRevA.98.022334

I. INTRODUCTION

Finite-dimensional discrete variables and infinite-dimensional continuous variables are two different ways of encoding quantum information [1,2]. Considerable progress has been made in quantum information processing for discrete variables [3–8] and continuous variables [9–14]. However, both encodings have their advantages and drawbacks [15,16]. In the discrete variable regime, the fidelities for preparing and operating quantum states are close to unity, but the events are always probabilistic. In the continuous variable regime, preparation and operation of quantum states are deterministic, but the states are very sensitive to loss. In this context the concept of hybrid entanglement is proposed. Hybrid entanglement combines the resource, operation, or measurement means of the discrete variable and continuous variable, and can accomplish some tasks which cannot be completed by a single coding style [17,18].

A lot of research work has been done in the field of hybrid entanglement [19–25]. Takeda *et al.* demonstrated deterministic teleportation of qubits by means of continuous variable teleportation [20]. They also realized entanglement swapping between discrete and continuous variables [21]. The generation of hybrid entanglement between a discrete variable qubit and a continuous variable coherent state is also a research spot in the field. Entanglement in the form of $|\psi\rangle = \frac{1}{\sqrt{2}}(|0\rangle|\alpha\rangle + |1\rangle|-\alpha\rangle)$ has been produced experimentally [24,25], where $|0\rangle$ is the vacuum state, $|1\rangle$ is the single-photon state, and $|\alpha\rangle$ is the coherent state with amplitude α. An increasingly important hybrid entanglement is in the form of $|\psi\rangle = \frac{1}{\sqrt{2}}(|H\rangle|\alpha\rangle + |V\rangle|-\alpha\rangle)$, where $|H\rangle$ and $|V\rangle$ are the single-photon states with horizontal (H) and vertical (V) polarizations, respectively. The polarized hybrid state can be used to perform deterministic quantum teleportation by using linear optics, and it is the necessary resource for universal gate operation [18]. A Bell inequality test using the polarized hybrid state can be highly robust against detection inefficiency [26]. In addition, the polarized hybrid state can be applied in a quantum repeater which can be purified by using a parity-check gate [27]. However, the generation of polarized hybrid entanglement has not been reported experimentally. In order to generate the polarized hybrid state, two obstacles must be overcome. One obstacle is that the first mode of the polarized hybrid state contains definitely one photon, so we cannot generate it by using adding photons [25] or subtracting photons [24]. The polarization of the photon from a polarized entangled photon pair is indeterminate, and can be H or V polarized. How to realize an effective interference and retain the polarization information at the same time is the other obstacle to generate the polarized hybrid state in experiment.

Recently Kwon and Jeong proposed a theoretical scheme to generate polarized hybrid entanglement [28]. A displacing operation is performed on one photon of a polarization entangled photon pair, then the displaced photon interferes with a fraction of the coherent state to erase "which path" information. Their application of displacing operation not only ensures that one photon is included in the first mode of the heralded hybrid state but also makes for a higher success probability. However, the polarization obstacle is still not solved. Based on Ref. [28], we propose a scheme to generate the polarized hybrid state in which the two obstacles can be overcome at the same time. We design two sets of interferences to erase which path information, the polarizations of which are H and V, respectively. The joint outputs of the two sets of interferences are used to herald the generation of the polarized hybrid state. We also analyze the effect of imperfect experimental conditions on the generated hybrid state, including inefficiency on-off single-photon detectors and available approximate resource states. In addition, we add the dark count noise of detectors in the theoretical model, and discuss the effect of dark noise on the fidelity of the heralded hybrid state.

*Corresponding author: wanghai@sxu.edu.cn

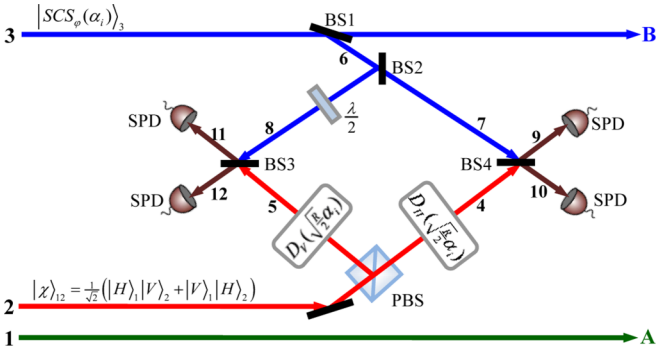

FIG. 1. Generation schematic diagram for polarized hybrid entanglement. $|\chi\rangle_{12}$, polarization entangled photon pairs; $|\mathrm{SCS}_\varphi(\alpha_i)\rangle_3$, superposition of coherent states; BS1, beam splitter with a small reflectivity; BS2-4, 50/50 beam splitters; PBS, polarized beam splitter; $D_H(\sqrt{\frac{R}{2}}\alpha_i)$ and $D_V(\sqrt{\frac{R}{2}}\alpha_i)$ are displacement operations with H and V polarizations, respectively; $\frac{\lambda}{2}$, half wave plate; SPDs, single-photon detectors.

II. GENERATION SCHEME

The ideal polarized hybrid entanglement is

$$|\Psi_\varphi(\alpha_f)\rangle_{\mathrm{AB}} = \frac{1}{\sqrt{2}}(|H\rangle_A|\alpha_f\rangle_B + e^{i\varphi}|V\rangle_A|-\alpha_f\rangle_B), \quad (1)$$

where φ is a relative phase factor. The generation schematic diagram is depicted in Fig. 1. Two resources are needed in the scheme: one is a polarization entangled photon pair, $|\chi\rangle_{12} = \frac{1}{\sqrt{2}}(|H\rangle_1|V\rangle_2 + |V\rangle_1|H\rangle_2)$, and the other is a superposition of coherent states (SCS), $|\mathrm{SCS}_\varphi(\alpha_i)\rangle_3 = N_\varphi(|\alpha_i\rangle_3 + e^{i\varphi}|-\alpha_i\rangle_3)$, where $N_\varphi = (2 + 2\cos\varphi e^{-2|\alpha_i|^2})^{-1/2}$ is the normalized coefficient.

We design two sets of interferences with perpendicular polarizations to overcome the polarization obstacle. One photon of the polarization entangled photon pair enters a polarized beam splitter to separate its H and V polarization components into two spatial modes. The polarization displacement operations are performed on the two modes as $D_{4H}(\sqrt{\frac{R}{2}}\alpha_i)D_{5V}(\sqrt{\frac{R}{2}}\alpha_i)(|1\rangle_{1H}|0\rangle_4|1\rangle_{5V} + |1\rangle_{1V}|1\rangle_{4H}|0\rangle_5)/\sqrt{2}$, and the subscripts "$H$" and "$V$" denote the polarization of the displacement operations and optical field state. The polarization of the input SCS state is definite, which is assumed to be H polarized. Passing through BS1 with a small reflectivity R, a coherent state $|\alpha\rangle_{3H}$ is transformed into $|\sqrt{R}\alpha\rangle_{6H}|\sqrt{T}\alpha\rangle_{\mathrm{BH}}$, where $T = 1 - R$ is the transmissivity of BS1. Then the reflected coherent state $|\sqrt{R}\alpha\rangle_{6H}$ is split into $|\sqrt{\frac{R}{2}}\alpha\rangle_{7H}|\sqrt{\frac{R}{2}}\alpha\rangle_{8H}$ by a 50:50 beam splitter BS2. A half wave plate is used to change the polarization of the light in mode 6 from H to V, so the state $|\mathrm{SCS}_\varphi(\alpha_i)\rangle_{3H}$ is changed into $N_\varphi(|\sqrt{\frac{R}{2}}\alpha_i\rangle_{7H}|\sqrt{\frac{R}{2}}\alpha_i\rangle_{8V}|\sqrt{T}\alpha_i\rangle_{\mathrm{BH}} + e^{i\varphi}|-\sqrt{\frac{R}{2}}\alpha_i\rangle_{7H}|-\sqrt{\frac{R}{2}}\alpha_i\rangle_{8V}|-\sqrt{T}\alpha_i\rangle_{\mathrm{BH}})$.

To entangle the polarization qubit and the SCS state, the displaced part of $|\chi\rangle_{12}$ is interfered with the reflected part of $|\mathrm{SCS}_\varphi(\alpha_i)\rangle_3$. The interferences with H and V polarization are carried on 50:50 beam splitters BS4 and BS3, respectively. After interference the state is evolved to

$$\begin{aligned}|\psi_\varphi\rangle = \frac{N_\varphi}{2}\{&|H\rangle_A|\sqrt{T}\alpha_i\rangle_B[|0\rangle_9|\sqrt{R}\alpha_i\rangle_{10}|1\rangle_{11}|\sqrt{R}\alpha_i\rangle_{12} + |0\rangle_9|\sqrt{R}\alpha_i\rangle_{10}|0\rangle_{11}D_{12}(\sqrt{R}\alpha_i)|1\rangle_{12}]\\ &+ e^{i\varphi}|H\rangle_A|-\sqrt{T}\alpha_i\rangle_B[|\sqrt{R}\alpha_i\rangle_9|0\rangle_{10}D_{11}(\sqrt{R}\alpha_i)|1\rangle_{11}|0\rangle_{12} + |\sqrt{R}\alpha_i\rangle_9|0\rangle_{10}|\sqrt{R}\alpha_i\rangle_{11}|1\rangle_{12}]\\ &+ |V\rangle_A|\sqrt{T}\alpha_i\rangle_B[|1\rangle_9|\sqrt{R}\alpha_i\rangle_{10}|0\rangle_{11}|\sqrt{R}\alpha_i\rangle_{12} + |0\rangle_9D_{10}(\sqrt{R}\alpha_i)|1\rangle_{10}|0\rangle_{11}|\sqrt{R}\alpha_i\rangle_{12}]\\ &+ e^{i\varphi}|V\rangle_A|-\sqrt{T}\alpha_i\rangle_B[D_9(\sqrt{R}\alpha_i)|1\rangle_9|0\rangle_{10}|\sqrt{R}\alpha_i\rangle_{11}|0\rangle_{12} + |\sqrt{R}\alpha_i\rangle_9|1\rangle_{10}|\sqrt{R}\alpha_i\rangle_{11}|0\rangle_{12}]\}. \end{aligned} \quad (2)$$

Four single-photon detectors are used to detect the output fields of the two sets of interferences. When the projection operator is chosen as

$$\prod = \mathrm{I}_A \otimes |0\rangle\langle 0|_9 \otimes |1\rangle\langle 1|_{10} \otimes |1\rangle\langle 1|_{11} \otimes |0\rangle\langle 0|_{12} \otimes \mathrm{I}_B, \quad (3)$$

the resulting density operator of the hybrid entanglement state between field modes A and B is

$$\rho = \frac{Tr_{9,10,11,12}[\prod|\psi_\varphi\rangle\langle\psi_\varphi|]}{\langle\psi_\varphi|\prod|\psi_\varphi\rangle} = |\Psi_\varphi(\alpha_f)\rangle\langle\Psi_\varphi(\alpha_f)|_{\mathrm{AB}}, \quad (4)$$

where $\alpha_f = \sqrt{T}\alpha_i$. From the analysis we can see that the ideal entangled state (1) can be generated by using this scheme. The success probability to herald the generation of hybrid entanglement is

$$P^\varphi = \langle\psi_\varphi|\prod|\psi_\varphi\rangle = \frac{N_\varphi^2}{2}\left(\frac{1}{T} - 1\right)\alpha_f^2 e^{-2(\frac{1}{T}-1)\alpha_f^2}. \quad (5)$$

Obviously, the success probability is relative to the hybrid state size α_f and the BS1 transmissivity T. We calculate the success probability in terms of α_f and T, as shown in Fig. 2. In the range of $\alpha_f \leqslant 2$, the success probability increases with decrease of T. For a given α_f, the success probability can be maximized to 4.6% when α_f is large enough. As is done in Ref. [28], we can choose the other measurement operation $\prod' = \mathrm{I}_A \otimes |1\rangle\langle 1|_9 \otimes |0\rangle\langle 0|_{10} \otimes |0\rangle\langle 0|_{11} \otimes |1\rangle\langle 1|_{12} \otimes \mathrm{I}_B$, and obtain a corresponding hybrid entanglement state $|\psi'\rangle_{\mathrm{AB}} = \frac{1}{\sqrt{2}}(|V\rangle_A|\alpha_f\rangle_B + e^{i\varphi}|H\rangle_A|-\alpha_f\rangle_B)$. So the total probability is $P^\varphi_{\mathrm{tot}} = 2P^\varphi$.

III. EXPERIMENTAL REALITY

A. Inefficient on-off single-photon detectors

In the above analysis, the quantum efficiencies of the single-photon detectors are assumed to be unity. However, the quantum efficiency of the detector is imperfect under current technology. Considering quantum efficiency, the "n

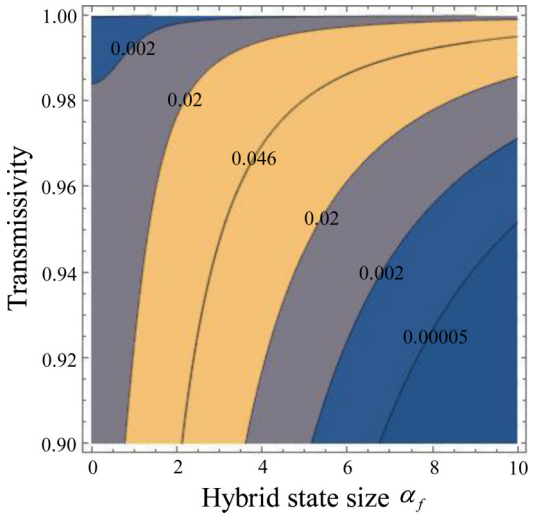

FIG. 2. Success probability of the polarized hybrid state in terms of its amplitude α_f and BS1 transmissivity T.

photons measurement event" by a single-photon detector can be described by the operator

$$\hat{E}_\eta^{(n)} = \sum_{m=0}^{\infty} C_{n+m}^m \eta^n (1-\eta)^m |n+m\rangle\langle n+m|, \tag{6}$$

where η is the quantum efficiency of detectors. The projection operator (3) is changed to

$$\begin{aligned}\Pi_\eta &= I_A \otimes \hat{E}_{\eta,9}^{(0)} \otimes \hat{E}_{\eta,10}^{(1)} \otimes \hat{E}_{\eta,11}^{(1)} \otimes \hat{E}_{\eta,12}^{(0)} \otimes I_B \\ &= \sum_{p=0}^{\infty}\sum_{q=0}^{\infty}\sum_{s=0}^{\infty}\sum_{t=0}^{\infty} qs\eta^2(1-\eta)^{p+q+s+t-2} \\ &\quad \times |p\rangle_9|q\rangle_{10}|s\rangle_{11}|t\rangle_{12}\langle t|_{12}\langle s|_{11}\langle q|_{10}\langle p|_9. \end{aligned} \tag{7}$$

The corresponding density operator of the heralded state is

$$\rho_\eta = \frac{Tr_{9,10,11,12}\left[\prod_\eta |\psi_\varphi\rangle\langle\psi_\varphi|\right]}{\langle\psi_\varphi|\prod_\eta|\psi_\varphi\rangle}. \tag{8}$$

The fidelity and success probability are

$$F_\eta^\varphi = {}_{\rm AB}\langle\psi_\varphi|\rho_\eta|\psi_\varphi\rangle_{\rm AB} = \tfrac{1}{2}\left[1+e^{-2(1-\eta)(\frac{1}{T}-1)\alpha_f^2}\right] \tag{9}$$

and

$$P_{\eta,\rm tot}^\varphi = 2\langle\psi_\varphi|\prod_\eta|\psi_\varphi\rangle = N_\varphi^2\eta^2\left(\frac{1}{T}-1\right)\alpha_f^2 e^{-2\eta(\frac{1}{T}-1)\alpha_f^2}, \tag{10}$$

respectively.

Now most commercial single-photon detectors cannot distinguish photon number, that is, the on-off detector. The detector will click, whether one photon is detected or multiple photons are detected. The "on" event of the on-off detector can be described by the operator

$$\hat{E}_\eta^{\rm on} = 1 - \sum_{m=0}^{\infty}(1-\eta)^m|m\rangle\langle m|, \tag{11}$$

where $\hat{E}_\eta^{\rm off} = \sum_{m=0}^{\infty}(1-\eta)^m|m\rangle\langle m|$ describes the event that no photon has been detected. Accordingly, the projection operator (3) is rewritten as

$$\begin{aligned}\Pi_\eta^{\rm on-off} &= I_A \otimes \hat{E}_{\eta,9}^{\rm off} \otimes \hat{E}_{\eta,10}^{\rm on} \otimes \hat{E}_{\eta,11}^{\rm on} \otimes \hat{E}_{\eta,12}^{\rm off} \otimes I_B \\ &= \sum_{p=0}^{\infty}\sum_{q=0}^{\infty}\sum_{s=0}^{\infty}\sum_{t=0}^{\infty}(1-\eta)^{p+t}[1-(1-\eta)^q] \\ &\quad \times [1-(1-\eta)^s]|p\rangle_9|q\rangle_{10}|s\rangle_{11}|t\rangle_{12}\langle t|_{12} \\ &\quad \times \langle s|_{11}\langle q|_{10}\langle p|_9. \end{aligned} \tag{12}$$

The corresponding density operator of the heralded state is

$$\rho_\eta^{\rm on-off} = \frac{Tr_{9,10,11,12}\left[\prod_\eta^{\rm on-off}|\psi_\varphi\rangle\langle\psi_\varphi|\right]}{\langle\psi_\varphi|\prod_\eta^{\rm on-off}|\psi_\varphi\rangle}. \tag{13}$$

The fidelity is

$$\begin{aligned}F_\eta^{\rm on-off} &= {}_{\rm AB}\langle\psi_\varphi|\rho_\eta^{\rm on-off}|\psi_\varphi\rangle_{\rm AB} \\ &= \frac{1}{2}\left[1+\frac{\eta\left(\frac{1}{T}-1\right)\alpha_f^2}{e^{(2-\eta)\left(\frac{1}{T}-1\right)\alpha_f^2}-e^{2(1-\eta)(\frac{1}{T}-1)\alpha_f^2}}\right]. \end{aligned} \tag{14}$$

The success probability is

$$\begin{aligned}P_{\eta,\rm tot}^{\rm on-off} &= 2\langle\psi_\varphi|\prod_\eta^{\rm on-off}|\psi_\varphi\rangle \\ &= N_\varphi^2\eta\left[e^{-\eta(\frac{1}{T}-1)\alpha_f^2}-e^{-2\eta(\frac{1}{T}-1)\alpha_f^2}\right]. \end{aligned} \tag{15}$$

Figure 3 shows the fidelity and success probability as a function of detection efficiency η and hybrid state size α_f. The imperfect detection efficiency η degrades the fidelity and reduces the success probability, while the large amplitude α_f brings down the fidelity and increases the success probability (in the range of $\alpha_f \leqslant 7$). In the case of photon-number-resolving detectors, the fidelity of the generated hybrid state

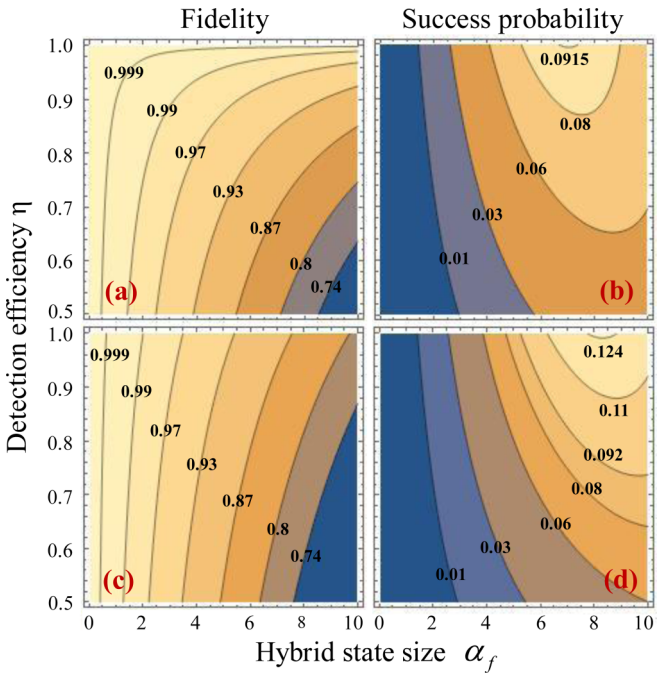

FIG. 3. (a), (c) Fidelity and (b), (d) success probability as a function of hybrid state size α_f and detection efficiency η. The photon-number-resolving and on-off detectors are used in the upper and lower figures, respectively.

can be close to unity as long as the detection efficiency is high enough at a given value of α_f. In the case of on-off detectors, the fidelity will be limited by the amplitude α_f. If one wants the fidelity to be greater than 99%, the amplitude α_f must be less than 2. Since on-off detectors cannot resolve the number of photons, the large amplitude α_f increases the chances of producing multiphoton states. So the large amplitude α_f causes the error probability increase and limits the fidelity.

B. Resources under realistic conditions

An odd SCS $[N_\pi(|\alpha\rangle - |-\alpha\rangle)]$ can be approximated by a photon-subtracted squeezed state, which has been demonstrated experimentally [29–32]. Under the basis of photon number states, a photon-subtracted squeezed state is expressed as

$$|\varphi_{ss}\rangle = \sum_{n=0}^{\infty} \frac{(\tanh s)^n \sqrt{(2n+1)!}}{(\cosh s)^{3/2} 2^n n!} |2n+1\rangle, \tag{16}$$

where s is the squeezing parameter. The fidelity between a photon-subtracted squeezed state and an odd SCS is [33,34]

$$F_{\alpha,s} = \frac{2\alpha^2 e^{\alpha^2(\tanh s - 1)}}{(\cosh s)^3 (1 - e^{-2\alpha^2})}. \tag{17}$$

For a given α, the fidelity is maximized when s satisfies

$$s = \operatorname{arccosh}\left(\sqrt{\frac{1}{2} + \frac{1}{6}\sqrt{9 + 4\alpha^4}}\right). \tag{18}$$

When the resources of photon-subtracted squeezed state $|\varphi_{ss}\rangle_3$ and polarization entangled photon pair $|\chi\rangle_{12}$ are used as input state, after interfering on BS3 and BS4 the state is evolved to

$$|\psi_{ss}\rangle = \frac{1}{\sqrt{2}} e^{-\frac{R}{2}|\alpha_i|^2} \sum_{k=0}^{\infty}\sum_{m=0}^{\infty}\sum_{n=0}^{\infty}\sum_{q=0}^{2n+1}\sum_{l}^{2n+1-q}\sum_{e=0}^{l}\sum_{g=0}^{2n+1-q-l} \frac{(\tanh s)^n \sqrt{(2n+1)!}\left(\sqrt{\frac{R}{2}}\alpha_i\right)^{k+m}(-1)^{2n+1-q-e-g}\kappa}{(\cosh s)^{3/2} 2^n n! \sqrt{k!}\sqrt{m!}}$$
$$\times \left\{ \begin{array}{l} +|H\rangle_A|q\rangle_B \sum_{f=0}^{k}\sum_{h=0}^{m+1} \sqrt{\frac{1}{2}(m+1)C_{m+1}^{f} C_k^h}\,|l-e+f\rangle_9|e+k-f\rangle_{10}|2n+1-q-l-g+h\rangle_{11}|g+m+1-h\rangle_{12} \\ -|H\rangle_A|q\rangle_B \sum_{f=0}^{k}\sum_{h=0}^{m} \sqrt{\frac{R}{2}}\alpha_i{}^* \sqrt{\frac{1}{2}(m+1)C_{m+1}^{f} C_k^h}\,|l-e+f\rangle_9|e+k-f\rangle_{10}|2n+1-q-l-g+h\rangle_{11}|g+m-h\rangle_{12} \\ +|V\rangle_A|q\rangle_B \sum_{f=0}^{m+1}\sum_{h=0}^{k} \sqrt{\frac{1}{2}(m+1)C_{m+1}^{f} C_k^h}\,|l-e+f\rangle_9|e+m+1-f\rangle_{10}|2n+1-q-l-g+h\rangle_{11}|g+k-h\rangle_{12} \\ -|V\rangle_A|q\rangle_B \sum_{f=0}^{m}\sum_{h=0}^{k} \sqrt{\frac{R}{2}}\alpha_i{}^* \sqrt{\frac{1}{2}(m+1)C_{m+1}^{f} C_k^h}\,|l-e+f\rangle_9|e+m-f\rangle_{10}|2n+1-q-l-g+h\rangle_{11}|g+k-h\rangle_{12} \end{array} \right\} \tag{19}$$

where $\kappa = \sqrt{C_{2n+1}^{q} T^q R^{2n+1-q} C_{2n+1-q}^{l} C_l^e C_{2n+1-q-l}^{g} (\frac{1}{2})^{4n+2-2q+m+k}}$, and the value of $\alpha_i = \sqrt{\frac{3}{2}\sinh 2s}$ is the equivalent amplitude of approximate SCS, which can be deduced from formula (18). The amplitude of the generated hybrid entanglement state can be expressed as $\alpha_f = \sqrt{\frac{3}{2}T\sinh 2s}$ when a photon-subtracted squeezed state is used as input. Generally a squeezed vacuum state is produced from an optical parametric oscillator (OPO). The squeezing parameter s depends on the pump parameter which is the ratio of the pump power to the threshold of the OPO cavity [35,36]. Hence one can adjust the pump power to control the squeezing parameter s, and then change the amplitude α_f. By using on-off detectors to herald the generation of the hybrid state, the density operator of the heralded state is

$$\rho_{ss}^{\text{on-off}} = \frac{Tr_{9,10,11,12}\left[\prod_\eta^{\text{on-off}} |\psi_{ss}\rangle\langle\psi_{ss}|\right]}{\langle\psi_{ss}| \prod_\eta^{\text{on-off}} |\psi_{ss}\rangle}. \tag{20}$$

The fidelity is calculated as

$$F_{ss}^{\text{on-off}} = {}_{\text{AB}}\langle\psi_\varphi|\rho_{ss}^{\text{on-off}}|\psi_\varphi\rangle_{\text{AB}}, \tag{21}$$

where the amplitude of the ideal hybrid state is taken to be $\sqrt{T}\alpha_i$. The success probability is

$$P_{ss,\text{tot}}^{\text{on-off}} = 2\langle\psi_{ss}| \prod_\eta^{\text{on-off}} |\psi_{ss}\rangle. \tag{22}$$

Figures 4(a) and 4(b) show the fidelity $F_{ss}^{\text{on-off}}$ and the success probability $P_{ss,\text{tot}}^{\text{on-off}}$ as a function of equivalent amplitude α_i of approximate SCS. The black solid line in Fig. 4(a) is the maximized fidelity $F_{\alpha_i,s}$ between a SCS and a photon-subtracted squeezed state. The dots, triangles, and squares in Figs. 4(a) and 4(b) denote fidelity $F_{ss}^{\text{on-off}}$ and success probability $P_{ss,\text{tot}}^{\text{on-off}}$ for $T = 0.99$, 0.95, and 0.90, respectively. For a small amplitude α_i, fidelity can be maintained at a very high level, and the BS1 transmissivity has little influence on it. The fidelity $F_{ss}^{\text{on-off}}$ with $\alpha_i = 0.7$ is 0.998, 0.993, and 0.988 for $T = 0.99$, 0.95, and 0.90, respectively. The curves of $F_{ss}^{\text{on-off}}$ have the same trend as those of $F_{\alpha_i,s}$ which decreases rapidly with α_i. The fidelity $F_{ss}^{\text{on-off}}$ with $T = 0.99$ varies from 0.99 to 0.86 by increasing α_i from 1 to 2. The success probability can be improved by one order of magnitude by changing the BS1 transmissivity from 0.99 to 0.90. So by choosing proper BS1 transmissivity one can acquire high fidelity and large heralding probability at the same time for a small amplitude α_i.

In quantum optical experiment, a polarization entangled photon pair is usually produced by a spontaneous parametric down conversion process (SPDC). The state from a SPDC

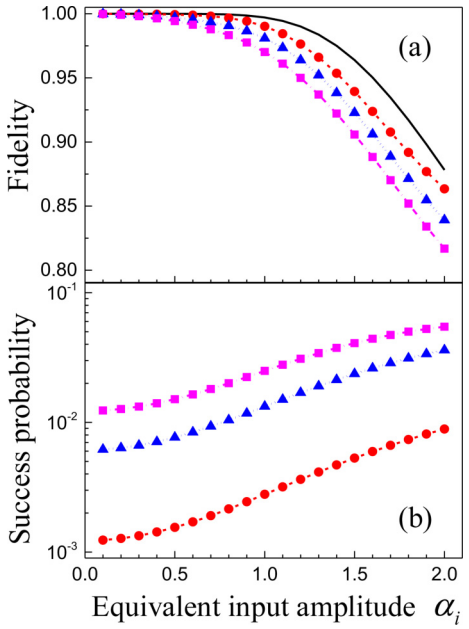

FIG. 4. (a) Fidelity and (b) success probability as a function of equivalent input amplitude α_i of approximate SCS. A photon-subtracted squeezed state is used to approximate a SCS. The black solid line in (a) represents maximized fidelities between SCSs and photon-subtracted squeezed states. The BS1 transmissivities are 0.99 (red dots), 0.95 (blue triangles), and 0.90 (pink squares), respectively.

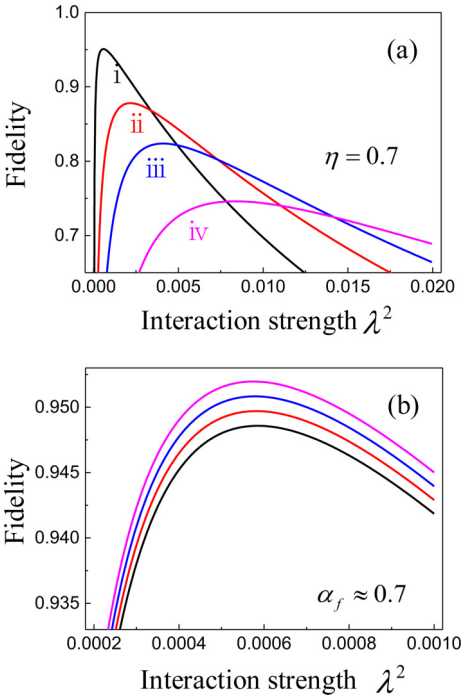

FIG. 5. Effective fidelity as a function of interaction strength λ^2 for different hybrid state size α_f (a) and for different detection efficiency η (b). (a) The hybrid state size $\alpha_f \approx 0.7$, 1.0, 1.2, and 1.5 for the lines i, ii, iii, and iv, respectively. (b) The detection efficiency $\eta = 0.9$, 0.7, 0.5, and 0.3 starting from the top, respectively. The BS1 transmissivity is 0.99 for both (a) and (b).

process can be given by the expression

$$|\mathrm{SPDC}_\lambda\rangle = \sqrt{1-\lambda^2}(|\phi_0\rangle_{12} + \lambda|\phi_1\rangle_{12} + \lambda^2|\phi_2\rangle_{12} + \cdots + \lambda^n|\phi_n\rangle_{12} + \cdots), \tag{23}$$

where λ is the interaction strength and $|\varphi_n\rangle_{12} = \frac{1}{\sqrt{1+n}}\sum_{m=0}^{n}|m\rangle_{1H}|n-m\rangle_{1V}|n-m\rangle_{2H}|m\rangle_{2V}$. In addition to the polarization entangled photon pairs $|\phi_1\rangle_{12}(|\chi\rangle_{12})$, the SPDC source also contains a vacuum state $|\phi_0\rangle_{12} = |0\rangle_{12}$, two-photon state $|\phi_2\rangle_{12} = \frac{1}{\sqrt{3}}(|2\rangle_{1V}|2\rangle_{2H} + |1\rangle_{1H}|1\rangle_{1V}|1\rangle_{2H}|1\rangle_{2V} + |2\rangle_{1H}|2\rangle_{2V})$, and multiphoton state $|\phi_n\rangle_{12}(n \geqslant 3)$. Because λ is small in the SPDC source, we only consider $|\phi_0\rangle$, $|\phi_1\rangle$, and $|\phi_2\rangle$, and all items $|\phi_n\rangle(n \geqslant 3)$ are thrown away in the following discussion.

If the input state in field modes 1 and 2 is a vacuum $|\phi_0\rangle$, the output of port A is also a vacuum. If the input state is $|\phi_2\rangle$, the output of port A is a two-photon state. Obviously, in both cases, the coincidence count of single-photon detectors will lead to a mistake for the generation of hybrid entanglement (1).Therefore, by using a SPDC source to generate polarization entangled photon pairs, the effective fidelity can be approximated written as

$$F_{\mathrm{SPDC}}^{\mathrm{eff}} = \frac{P_1}{\lambda^{-2}P_0 + P_1 + \lambda^2 P_2} F_{ss}^{\mathrm{on-off}} \tag{24}$$

where P_0, P_1, and P_2 are the success probabilities using $|\varphi_0\rangle$, $|\varphi_1\rangle$, and $|\varphi_2\rangle$ as the input states, respectively.

We calculate the fidelity as a function of interaction strength λ^2, as shown in Fig. 5. In the calculation, the BS1 transmissivity is 99%. The curves i, ii, iii, and iv in Fig. 5(a) represent the effective fidelity for $\alpha_f \approx 0.7$, 1.0, 1.2, and 1.5, respectively, by taking detection efficiency $\eta = 0.7$. For a given α_f, there is an optimal value of λ^2 to maximize the effective fidelity. For $\alpha_f \approx 0.7$, the peak effective fidelity is 95.1% with $\lambda^2 = 6.5\times10^{-4}$. By increasing the amplitude α_f from 0.7 to 1.5, the peak effective fidelity decreases from 95.1 to 74.6%. In Fig. 5(b) we show the effective fidelity for different detection efficiencies. The maximized effective fidelity reduces from 95.2 to 94.8% when the detection efficiency varies from 0.9 to 0.3. So detection efficiency has little effect on effective fidelity.

C. Dark count noise of single-photon detectors

The generation of the hybrid entanglement state is heralded by performing coincidence measurement on the single-photon detectors. Due to the intrinsic probabilistic of hybrid state generation and small appearance probability of polarization entangled photon pairs in a SPDC source, the heralding probability of the hybrid state is considerably low. The dark counts of single-photon detectors will inevitably degrade the fidelity of the heralded hybrid state.

Considering dark counts of a single-photon detector, the "on" event of the on-off detector with quantum efficiency η can be described as the operator [37]

$$\hat{E}_{\eta,\nu}^{\mathrm{on}} = \hat{I} - \hat{E}_{\eta,\nu}^{\mathrm{off}} \tag{25}$$

where ν is the dark count rate, and $\hat{E}_{\eta,\nu}^{\mathrm{off}} = e^{-\nu}\sum_{m=0}^{\infty}(1-\eta)^m|m\rangle\langle m|$ is the operator describing the "off" event of the detector. The projection operator (3) can be

TABLE I. Success probabilities of $P_{0\nu}$, $P_{1\nu}$, and $P_{2\nu}$ for different dark count rates. The squeezing parameter $s = 0.161$ ($\alpha_i = 0.7$), BS1 transmissivity $T = 0.99$, and detection efficiency $\eta = 0.7$.

ν	$P_{0\nu}$	$P_{1\nu}$	$P_{2\nu}$
0	2.75×10^{-8}	1.91×10^{-3}	8.21×10^{-2}
10^{-7}	2.86×10^{-8}	1.91×10^{-3}	8.21×10^{-2}
10^{-6}	3.84×10^{-8}	1.91×10^{-3}	8.21×10^{-2}
10^{-5}	1.37×10^{-7}	1.92×10^{-3}	8.21×10^{-2}
10^{-4}	1.14×10^{-6}	1.98×10^{-3}	8.22×10^{-2}

expressed as

$$\begin{aligned}\Pi_{\eta,\nu}^{\text{on-off}} &= I_A \otimes \hat{E}_{\eta,\nu,9}^{\text{off}} \otimes \hat{E}_{\eta,\nu,10}^{\text{on}} \otimes \hat{E}_{\eta,\nu,11}^{\text{on}} \otimes \hat{E}_{\eta,\nu,12}^{\text{off}} \otimes I_B \\ &= \sum_{p=0}^{\infty}\sum_{q=0}^{\infty}\sum_{s=0}^{\infty}\sum_{t=0}^{\infty} e^{-2\nu}(1-\eta)^{p+t}[1-e^{-\nu}(1-\eta)^q] \\ &\quad \times [1-e^{-\nu}(1-\eta)^s]|p\rangle_9|q\rangle_{10}|s\rangle_{11}|t\rangle_{12} \\ &\quad \times \langle t|_{12}\langle s|_{11}\langle q|_{10}\langle p|_9. \end{aligned} \tag{26}$$

The effective fidelity can be approximated by the following expression:

$$F_{\text{SPDC},\nu}^{\text{eff}} = \frac{P_1}{\lambda^{-2}P_{0\nu} + P_{1\nu} + \lambda^2 P_{2\nu}} F_{ss}^{\text{on-off}} \tag{27}$$

where $P_{0\nu}$, $P_{1\nu}$, and $P_{2\nu}$ are the success probabilities with dark counts when $|\phi_0\rangle$, $|\phi_1\rangle$, and $|\phi_2\rangle$ are used as input states, respectively. By using the projection operator the heralding probabilities can be acquired, for example, $P_{1\nu} = 2\langle\psi_{ss}|\prod_{\eta,\nu}^{\text{on-off}}|\psi_{ss}\rangle$.

Next, we will examine the effect of dark counts on the probabilities of $P_{0\nu}$, $P_{1\nu}$, and $P_{2\nu}$. Under the condition of $s = 0.161$, $T = 0.99$, and $\eta = 0.7$, we calculate the probabilities for different dark count rates, and the results are shown in Table I. When dark count rate ν increases from 10^{-7} to 10^{-4}, $P_{1\nu}$ increases slightly, $P_{2\nu}$ basically remains unchanged, while $P_{0\nu}$ increases by one order of magnitude. So we can infer that the influence of the dark counts on $P_{0\nu}$ is the main reason for the degradation of effective fidelity. The maximized effective fidelities with optimal interaction strength λ^2 are also calculated for different dark count rates, as shown in Fig. 6. The black dots are the maximized effective fidelities $F_{\text{SPDC}}^{\text{eff}}$ without dark counts. If the dark count rate is small enough ($\nu < 10^{-6}$), the effective fidelity $F_{\text{SPDC},\nu}^{\text{eff}}$ is almost not affected by the dark counts. With a higher squeezing parameter or a lower BS1 transmissivity, the effective fidelity has a better tolerance for the dark counts. A high squeezing parameter means a large mean photon number in the photon-subtracted squeezed state, which results in large P_0. So the influence of the dark count on $P_{0\nu}$ is small, and the fidelity decreases slowly with the increase of the dark count. Similarly, in the case of a lower transmissivity, a larger fraction of the photon-subtracted squeezed state is reflected and participates in interference, which also results in higher p_0 and makes effective fidelity insensitive to the dark counts. When the squeezed parameter is 0.161 ($\alpha_f \approx 0.7$) and the BS transmissivity is 0.95, the effective fidelity is 0.92 with a dark count rate of 10^{-5}. When the squeezed parameter is 0.313 ($\alpha_f \approx 1$), the effective fidelity can be maintained at more than 0.85 with a dark count rate of 10^{-5}.

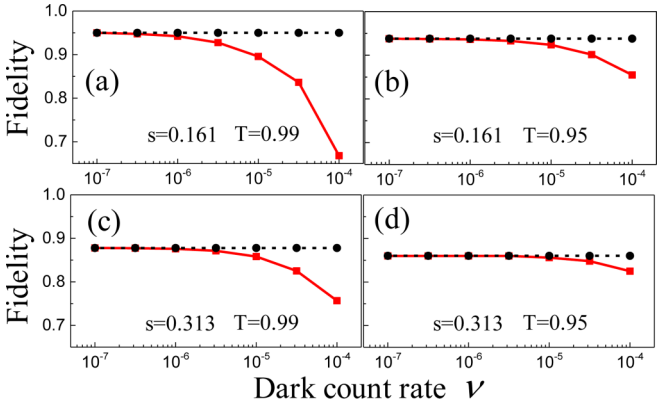

FIG. 6. Effective fidelity as a function of dark count rate for different squeezing parameters and BS1 transmissivities. The detection efficiency is 0.7.

IV. CONCLUSIONS

We propose an experimentally feasible scheme to realize hybrid entanglement between a polarization qubit and a coherent state. Two sets of interferences with perpendicular polarizations are designed to erase which path information. The joint outputs of the two sets of interferences are used to herald the generation of the hybrid state. We calculate success probability and fidelity of the heralded hybrid state under imperfect experimental conditions, including inefficient on-off single-photon detectors and available approximate resource states. In addition, we consider the effect of the dark count rate of detectors on the fidelity. Under the actual experimental condition, the fidelity of the heralded state can reach 0.92 with a squeezed parameter of 0.161 ($\alpha_f \approx 0.7$) and dark count rate of 10^{-5}.

The hybrid state is obtained from a photon-subtracted squeezed state, and its amplitude is related to the squeezing parameter s which can be controlled by the pump power of the OPO cavity in experiment. In our scheme the amplitude of the generated hybrid state with high fidelity is small. This is largely due to two reasons.

(1) A photon-subtracted squeezed state is used as the approximate source, which can be treated as a SCS with high fidelity for small amplitude of coherent state ($\alpha \leqslant 1.2$).

(2) The on-off single-photon detectors limit the fidelity of the generated hybrid state with large amplitude. No matter how much the detection efficiency is, the fidelity of the generated hybrid state will not exceed 0.99 with $\alpha_f \geqslant 2$.

To acquire the hybrid entanglement state with large amplitude, one should first produce SCS with large amplitude, which can be realized by amplifying SCS [33,38] or a "cat breeding" operation [39,40]. In addition, photon number resolving single-photon detectors must be used to herald generation of the hybrid state.

ACKNOWLEDGMENTS

This work was supported by the Key Project of the Ministry of Science and Technology of China (Grant No. 2016YFA0301402), and by the National Natural Science Foundation of China (Grants No. 11475109, No. 11834010, and No. 11604191).

[1] P. Kok, W. J. Munro, K. Nemoto, T. C. Ralph, J. P. Dowling, and G. J. Milburn, Rev. Mod. Phys. **79**, 135 (2007).

[2] S. L. Braunstein and P. van Loock, Rev. Mod. Phys. **77**, 513 (2005).

[3] D. Bouwmeester, J.-W. Pan, K. Mattle, M. Eibl, H. Weinfurter, and A. Zeilinger, Nature (London) **390**, 575 (1997).

[4] L.-M. Duan, M. D. Lukin, J. I. Cirac, and P. Zoller, Nature (London), **414**, 413 (2001).

[5] X.-C. Yao, T.-X. Wang, P. Xu, H. Lu, G.-S. Pan, X.-H. Bao, C.-Z. Peng, C.-Y. Lu, Y.-A. Chen, and J.-W. Pan, Nat. Photon. **6**, 225 (2012).

[6] K. S. Choi, A. Goban, S. B. Papp, S. J. van Enk, and H. J. Kimble, Nature (London) **468**, 412 (2010).

[7] W. Zhang, D.-S. Ding, M.-X. Dong, S. Shi, K. Wang, S.-L. Liu, Y. Li, Z.-Y. Zhou, B.-S. Shi, and G.-C. Guo, Nat. Commun. **7**, 13514 (2016).

[8] Y.-F. Pu, N. Jiang, W. Chang, H.-X. Yang, C. Li, and L.-M. Duan, Nat. Commun. **8**, 15359 (2017).

[9] A. Furusawa, J. L. Sørensen, S. L. Braunstein, C. A. Fuchs, H. J. Kimble, and E. S. Polzik, Science **282**, 706 (1998).

[10] P. van Loock, C. Weedbrook, and M. Gu, Phys. Rev. A **76**, 032321 (2007).

[11] S. Pirandola, J. Eisert, C. Weedbrook, A. Furusawa, and S. L. Braunstein, Nat. Photon. **9**, 641 (2015).

[12] H. Krauter, D. Salart, C. A. Muschik, J. M. Petersen, H. Shen, T. Fernholz, and E. S. Polzik, Nat. Phys. **9**, 400 (2013).

[13] S. Yokoyama, R. Ukai, S. C. Armstrong, C. Sornphiphatphong, T. Kaji, S. Suzuki, J. Yoshikawa, H. Yonezawa, N. C. Menicucci, and A. Furusawa, Nat. Photon. **7**, 982 (2013).

[14] X.-L. Su, S.-H. Hao, X.-W. Deng, L.-Y. Ma, M.-H. Wang, X.-J. Jia, C.-D. Xie, and K.-C. Peng, Nat. Commun. **4**, 2828 (2013).

[15] K. Park and H. Jeong, Phys. Rev. A **82**, 062325 (2010).

[16] J. B. Brask, I. Rigas, E. S. Polzik, U. L. Andersen, and A. S. Sørensen, Phys. Rev. Lett. **105**, 160501 (2010).

[17] P. van Loock, Laser Photon. Rev. **5**, 167 (2011).

[18] S.-W. Lee and H. Jeong, Phys. Rev. A **87**, 022326 (2013).

[19] K. Kreis and P. van Loock, Phys. Rev. A **85**, 032307 (2012).

[20] S. Takeda, T. Mizuta, M. Fuwa, P. van Loock, and A. Furusawa, Nature (London) **500**, 315 (2013).

[21] S. Takeda, M. Fuwa, P. van Loock, and A. Furusawa, Phys. Rev. Lett. **114**, 100501 (2015).

[22] A. Tiranov, J. Lavoie, P. C. Strassmann, N. Sangouard, M. Afzelius, F. Bussières, and N. Gisin, Phys. Rev. Lett. **116**, 190502 (2016).

[23] O. Morin, J.-D. Bancal, M. Ho, P. Sekatski, V. D'Auria, N. Gisin, J. Laurat, and N. Sangouard, Phys. Rev. Lett. **110**, 130401 (2013).

[24] O. Morin, K. Huang, J.-L. Liu, H. L. Jeannic, C. Fabre, and J. Laurat, Nat. Photon. **8**, 570 (2014).

[25] H. Jeong, A. Zavatta, M. Kang, S.-W. Lee, L. S. Costanzo, S. Grandi, T. C. Ralph, and M. Bellini, Nat. Photon. **8**, 564 (2014).

[26] H. Kwon and H. Jeong, Phys. Rev. A **88**, 052127 (2013).

[27] Y.-B. Sheng, L. Zhou, and G.-L. Long, Phys. Rev. A **88**, 022302 (2013).

[28] H. Kwon and H. Jeong, Phys. Rev. A **91**, 012340 (2015).

[29] J. S. Neergaard-Nielsen, B. M. Nielsen, C. Hettich, K. Mølmer, and E. S. Polzik, Phys. Rev. Lett. **97**, 083604 (2006).

[30] K. Wakui, H. Takahashi, A. Furusawa, and M. Sasaki, Opt. Express **15**, 3568 (2007).

[31] J. Wenger, R. Tualle-Brouri, and P. Grangier, Phys. Rev. Lett. **92**, 153601 (2004).

[32] T. Gerrits, S. Glancy, T. S. Clement, B. Calkins, A. E. Lita, A. J. Miller, A. L. Migdall, S. W. Nam, R. P. Mirin, and E. Knill, Phys. Rev. A **82**, 031802(R) (2010).

[33] A. P. Lund, H. Jeong, T. C. Ralph, and M. S. Kim, Phys. Rev. A **70**, 020101(R) (2004).

[34] M. S. Kim, E. Park, P. L. Knight, and H. Jeong, Phys. Rev. A **71**, 043805 (2005).

[35] M. Mehmet, S. Ast, T. Eberle, S. Steinlechner, H. Vahlbruch, and R. Schnabel, Opt. Express **19**, 25763 (2011).

[36] Y.-S. Han, X. Wen, J. He, B.-D. Yang, Y.-H. Wang, and J.-M. Wang, Opt. Express **24**, 2350 (2016).

[37] S. Suzuki, K. Tsujino, F. Kannari, and M. Sasaki, Opt. Commun. **259**, 758 (2006).

[38] A. Laghaout, J. S. Neergaard-Nielsen, I. Rigas, C. Kragh, A. Tipsmark, and U. L. Andersen, Phys. Rev. A **87**, 043826 (2013).

[39] A. Ourjoumtsev, H. Jeong, R. Tualle-Brouri, and P. Grangier, Nature (London) **448**, 784 (2007).

[40] J. Etesse, M. Bouillard, B. Kanseri, and R. Tualle-Brouri, Phys. Rev. Lett. **114**, 193602 (2015).